

Discovery and pre-clinical development of AKY-1189, a potent and selective Nectin-4 miniprotein binder optimized for use as a targeted radiopharmaceutical



James Way¹, William Blackwell¹, Andrew Clay¹, Marci Copeland¹, Michael Doligalski¹, Isaiah Gober¹, Hyun Joo Kil¹, Tatsiana Kosciuk¹, Daša Lipovšek², Wai Lau², Mehran Makvandi¹, Iris Paulus¹, Trevor Price¹, Howard Sauls¹, Srividhya Subramanian², Erin Swiger¹, Mark Woodward¹, Jeffrey Kovacs¹, Paul Feldman¹

Aktis Oncology, Discovery and Preclinical Translation, Durham NC, USA¹ and Boston MA, USA².

INTRODUCTION

- Miniproteins are an ideal targeting chemotype for radiopharmaceuticals due to their ability to fold into diverse three-dimensional structures, their potent and selective binding to a variety of targets, and their small size that facilitates rapid clearance and deep tumor penetration.
- The “fast-in, fast-out” pharmacokinetics and selectivity of miniproteins, combined with the extremely potent but short-range energy emissions of α -particles, help minimize side effects and drive robust efficacy.
- Nectin-4 is a promising target for precision radiopharmaceutical development given its restricted normal tissue expression profile in adults and its overexpression in 55% to 90% of urothelial, breast, lung, head/neck, and cervical tumors.¹⁻⁴

DISCOVERY

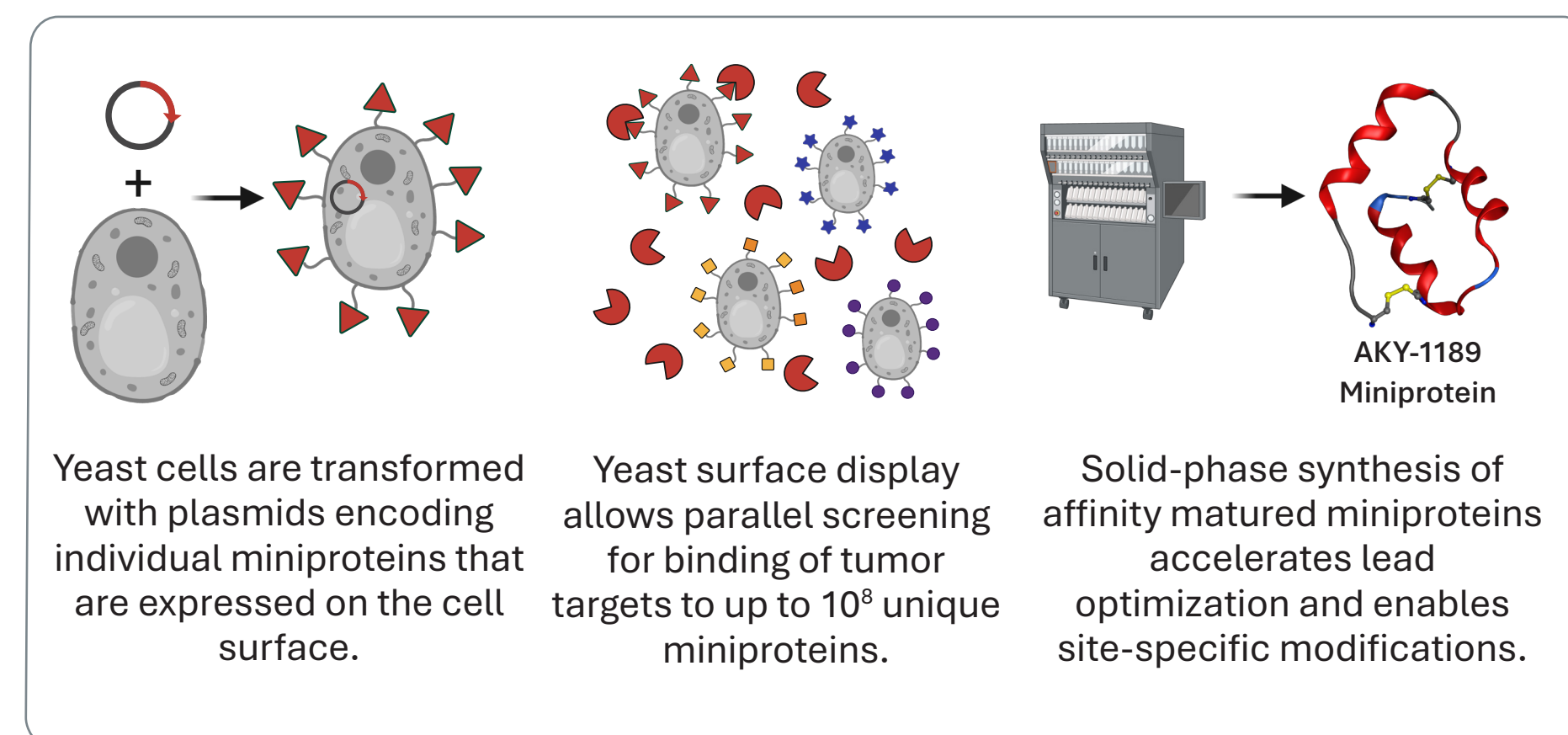


Figure 1. Yeast-surface-display (YSD) platform and solid phase miniprotein synthesis supports lead optimization.

Identification of High-Affinity Miniprotein Binders to Nectin-4

- Affinity maturation coupled with subsequent rounds of medicinal chemistry optimization and characterization (affinity, selectivity, physicochemical properties) led to the discovery of candidate molecules with improved properties.

Stage	K_D (nM)	Off Rate (sec^{-1})
Original Hit	47,000	0.130
Affinity matured miniprotein 1	90	0.016
Affinity matured miniprotein 2	9.7	0.025
Lead ¹	5.8	0.020
Optimized exemplar miniprotein ^{1,2}	3.0	0.005
AKY-1189 ^{1,2}	0.22	0.001

Table 1. Affinities of synthesized miniproteins.
¹ Specificity was validated using Retrogenix Cell Microarray Technology.
² Molecule was optimized using medicinal chemistry.

AKY-1189 Binds Nectin-4 With High Affinity In Vitro and On Cells

- Biotin-AKY-1189 binds recombinant human Nectin-4 with an observed K_D of 0.22 nM when assessed by surface plasmon resonance (SPR) (**Figure 2A**).
- On-cell binding of biotin-AKY-1189 to Nectin-4 was demonstrated on HT-1376 human urothelial carcinoma cells with an observed K_D of 0.82 nM as assessed by a competitive binding assay (DELFA) (**Figure 2B**).

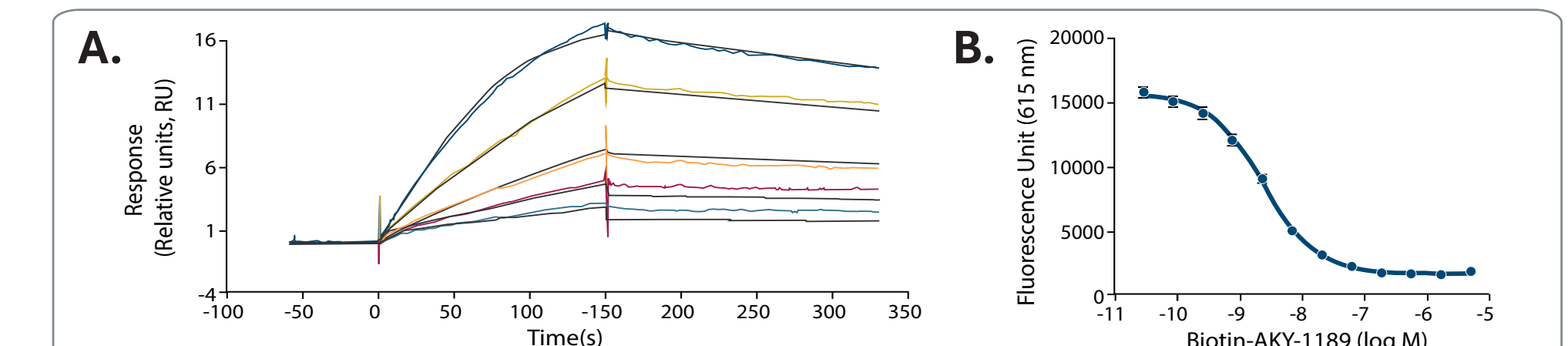


Figure 2. Biotin-AKY-1189 binding to Nectin-4. **A.** SPR binding of biotin-AKY-1189 to recombinant human Nectin-4 protein. **B.** Dose-response curve of biotin-AKY-1189 binding to Nectin-4 endogenously expressed on HT-1376 human urothelial cancer cells.

CHARACTERIZATION

AKY-1189 Selectively Binds Nectin-4 on Cancer Cells

- Nectin-4 CRISPR/Cas9-mediated knockout (KO) in HT-1376 cells was confirmed via flow cytometry (**Figure 3A**).
- Biotin-AKY-1189 demonstrates on-target binding to cell surface Nectin-4 *in vitro* (**Figure 3B, C**).
- Biotin-AKY-1189 does not bind Nectin-4 CRISPR/Cas9 KO cells (**Figure 3B, C**).

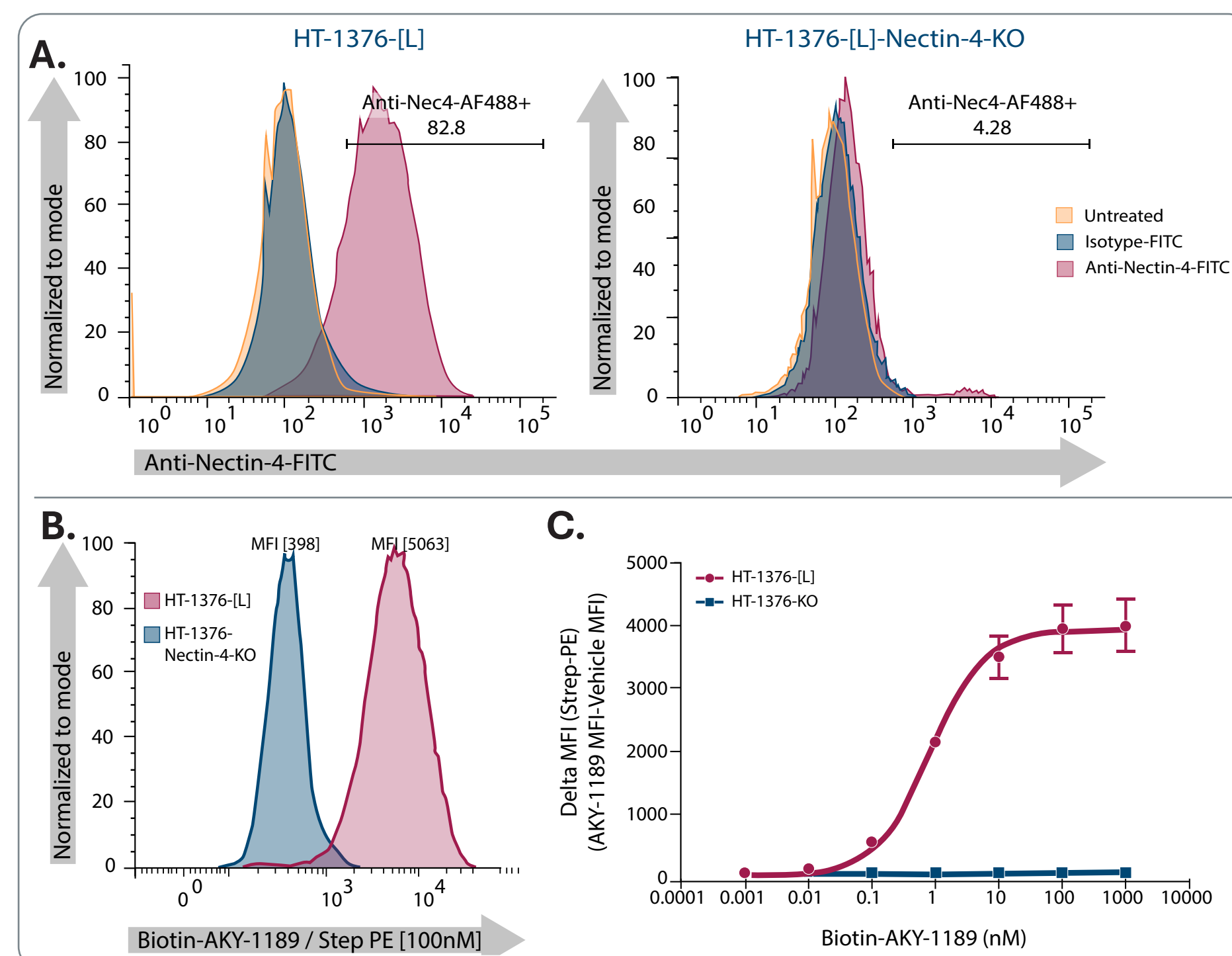


Figure 3. On-cell *in vitro* target selectivity of biotin-AKY-1189. **NOTE: Specificity of biotin-AKY-1189 binding to Nectin-4 was additionally verified across 6200+ human cell surface and secreted proteins using Retrogenix Cell Microarray Technology with >450-fold selectivity over demonstrated K_D .**

AKY-1189 Is Rapidly Internalized After Binding to Cell Surface Nectin-4

- AKY-1189 potently and selectively binds endogenous Nectin-4 on the surface of HT-1376 cells and is rapidly internalized after 30 minutes (**Figure 4A**, white arrows) but is not bound or internalized in Nectin-4 KO cells (**Figure 4B**).

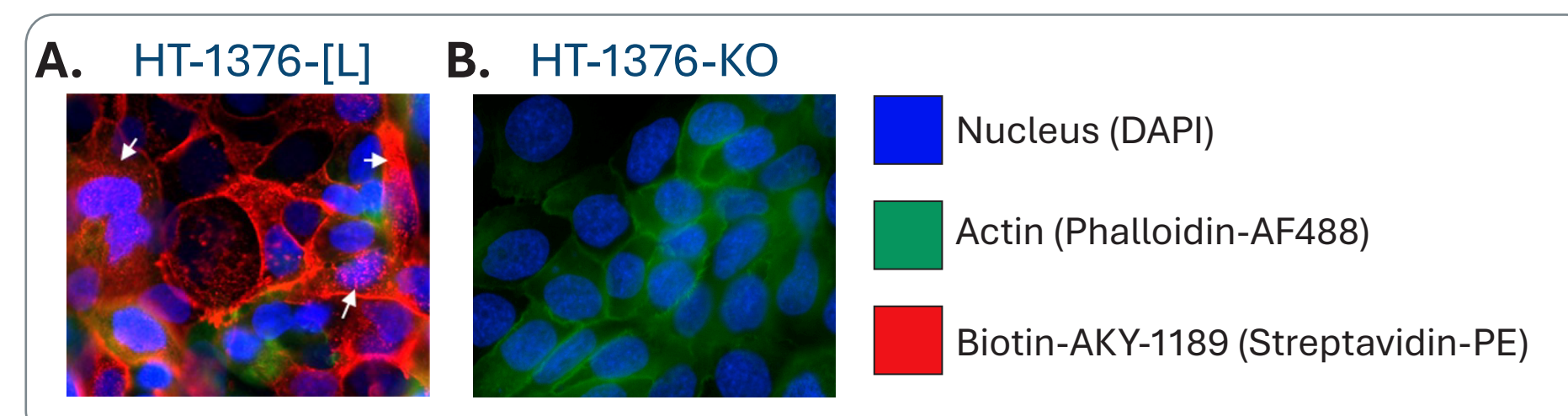


Figure 4. Immunofluorescent images of biotin-AKY-1189 imaged with a Streptavidin-PE conjugate in HT-1376-[L] wild type (A) and Nectin-4 KO (B) cells.

AKY-1189 Is Rapidly Cleared from the Plasma In Vivo

- Pharmacokinetic (PK) profile of In-AKY-1189 demonstrates “fast-in, fast-out” kinetics with near dose proportionality and plasma clearance at glomerular filtration rate (GFR) (**Figure 5**) in rats after a single dose.

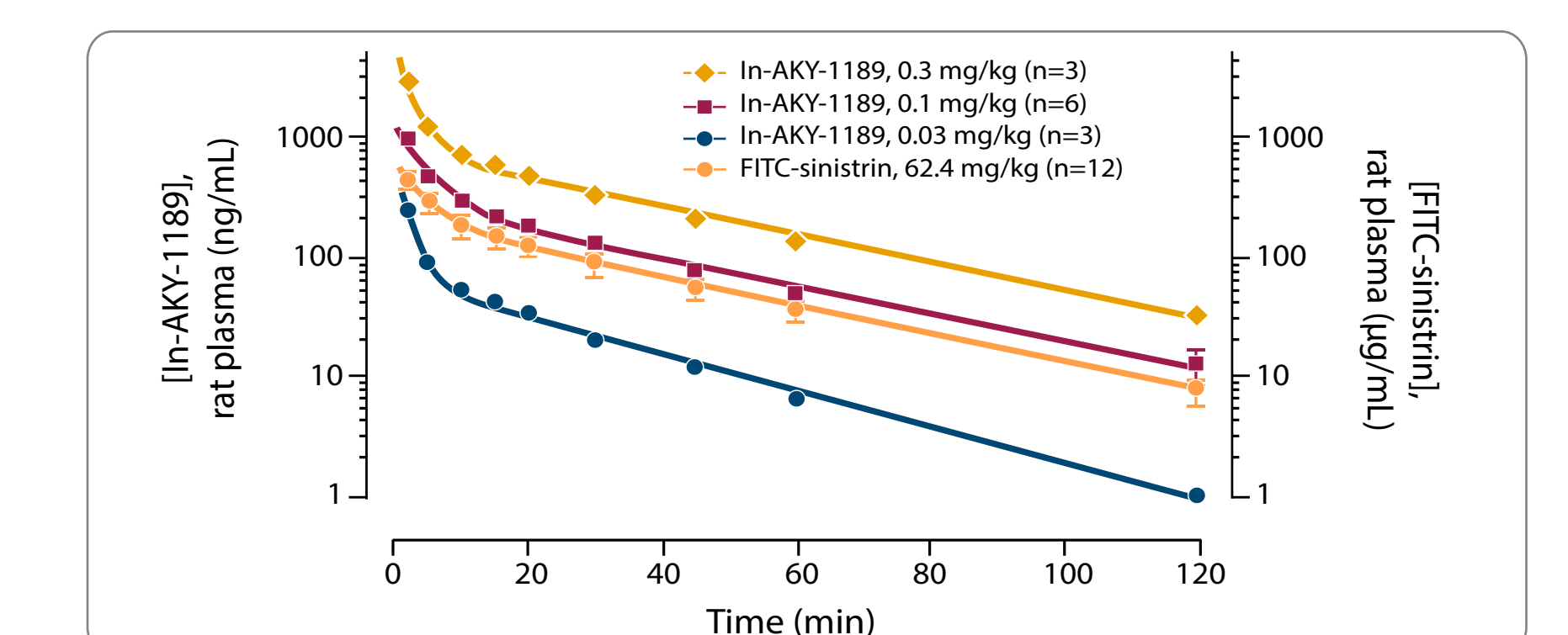


Figure 5. Pharmacokinetic profile of In-AKY-1189 in Sprague-Dawley rats after single-dose intravenous administration. FITC-sinistrin was co-formulated with In-AKY-1189 as a control molecule that is cleared at GFR.⁵

Dose (mg/kg)	N	$T_{1/2}$ (min)	AUC_{INF} ($\text{min} \cdot \text{ng/mL}$)	CL (mL/min/kg)	V_{SS} (mL/kg)
0.03	3	20.9 (1.8)	2850 (229)	10.6 (0.9)	202 (24)
0.1	6	26.4 (3.5)	15009 (1263)	6.9 (0.5)	182 (8.3)
0.3	3	26.5 (0.9)	41017 (2015)	7.3 (0.4)	199 (24)
62.4*	12	26.6 (17)	8.79e6 (6.1e5)	7.4 (0.4)	222 (9.9)

Table 3. Plasma pharmacokinetic profile of In-AKY-1189 (top three rows). Noncompartmental analysis reported values \pm standard error. *Bottom row shows analysis for co-administered FITC-sinistrin.

IN VIVO BIODISTRIBUTION AND EFFICACY

Translational Relevance of Cell Line-Derived Xenograft (CDX) Models

- HT-1376 CDX models endogenously or exogenously expressing Nectin-4 were evaluated via immunohistochemistry and categorized as Low (H-score = 175) and Representative (H-score = 291) (**Figure 6A, B**) given that the median H-score for patients with metastatic urothelial carcinoma is 280⁶ (patient biopsy shown; H-score = 286) (**Figure 6C**).

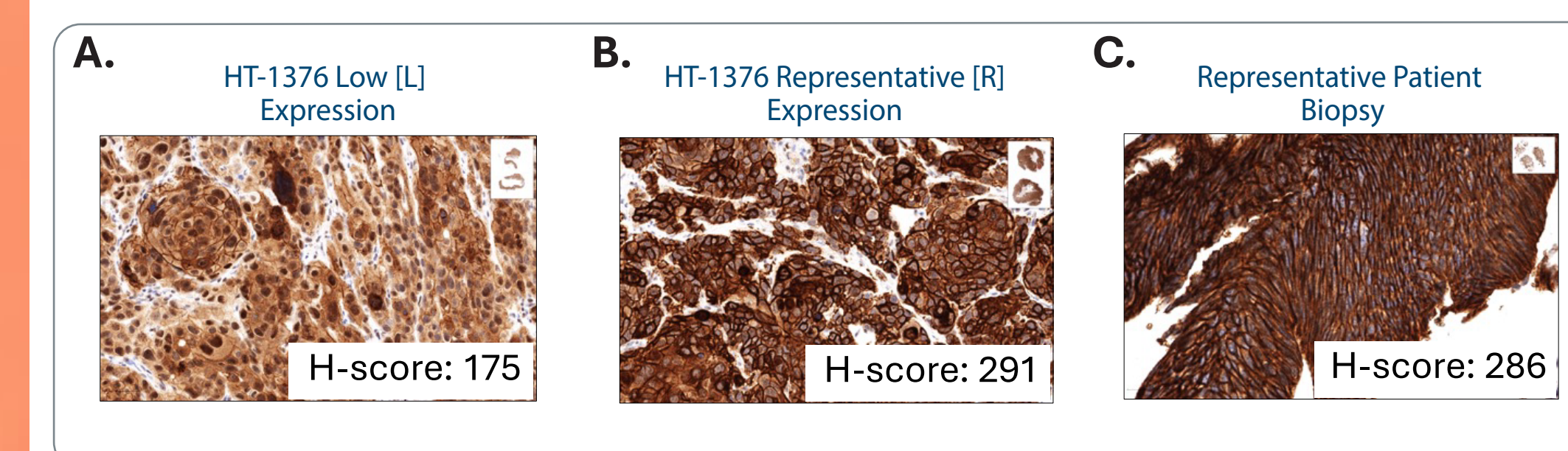


Figure 6. Immunohistochemical analysis of expression of cell surface Nectin-4. Exemplar low expression (A) and representative expression (B) in HT-1376 CDX sections. C. Representative patient biopsy.

²²⁵Ac-AKY-1189 Demonstrates Target-Dependent Efficacy and Survival Benefit After a Single Administration

- ²²⁵Ac-AKY-1189 drives robust anti-tumor effects *in vivo* after a single administration of drug in both the HT-1376-[L] and HT-1376-[R] models (**Figure 8A**) with no impacts on animal weights (**Figure 8B**), suggesting a well-tolerated therapeutic dose.
- A prolonged survival benefit was observed (**Figure 8C, Table 4**) in both models, suggesting a spectrum of Nectin-4-expressing patients who may benefit.

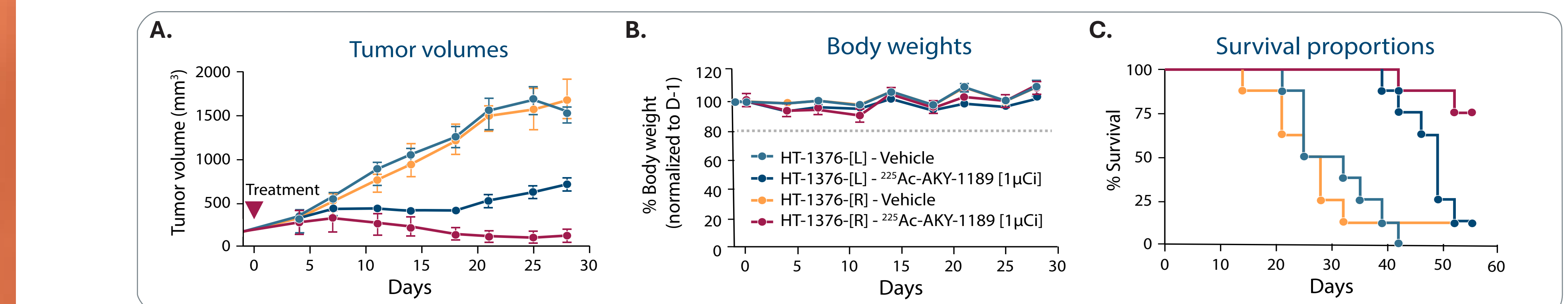


Figure 8. Preclinical efficacy of ²²⁵Ac-AKY-1189 in mouse models of metastatic urothelial carcinoma. Tumor volumes (A) and body weights (B) measured bi-weekly. C. Survival proportions over 55 days. Animals were treated with a single administration of ²²⁵Ac-AKY-1189 at 1 μCi of activity or vehicle.

Model	Treatment	Median survival (Days)	Significance (Gehan-Breslow-Wilcoxon test)
HT-1376-[L]	Vehicle	28.5	p=0.0006
	²²⁵ Ac-AKY-1189	49.0	
HT-1376-[R]	Vehicle	26.5	p=0.0017
	²²⁵ Ac-AKY-1189	Not Reached	

Table 4. Survival benefit analysis for ²²⁵Ac-AKY-1189-treated animals.

²²⁵Ac-AKY-1189 Demonstrates Improved Anti-Tumor Activity Compared to Enfortumab Vedotin in a Model of Urothelial Cancer

- A single administration of ²²⁵Ac-AKY-1189 drives greater anti-tumor effects than 3 administrations of enfortumab vedotin (EV) in HT-1376-[L] xenografts (**Figure 9A**) at well-tolerated dosing regimens (**Figure 9B**).
- Exposures of EV were optimized to align with plasma exposures achieved in patients at the approved clinical doses of EV (**Figure 9C and table inset**).

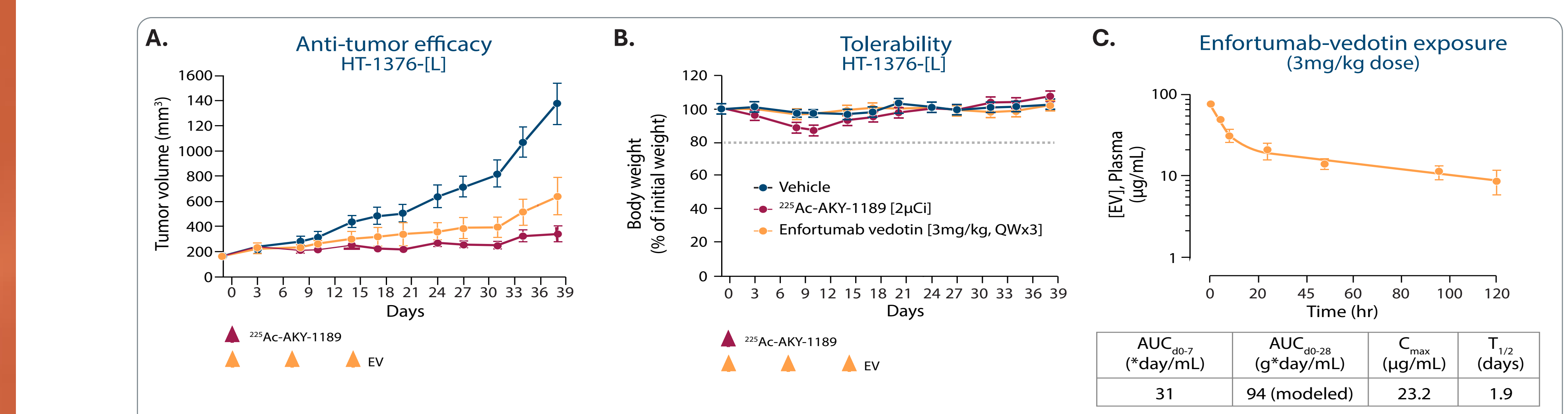


Figure 9. Animals received ²²⁵Ac-AKY-1189 [2 μCi] at Day 0 as a single bolus intravenous (IV) administration or enfortumab vedotin (EV) as an IV injection (3 mg/kg, QWx3). Tumor volumes (A) and body weights (B) were measured bi-weekly for 4 weeks. C. Plasma exposures of EV were measured in mice via LC/MS/MS and parameters calculated; clinical exposure (AUC_{0-28}) of the approved dose of EV is $111 \pm 38 \mu\text{g} \cdot \text{day/mL}$.

AUC_{0-7} ($^* \mu\text{g} \cdot \text{day/mL}$)	AUC_{0-28} ($\text{g} \cdot \text{day/mL}$)	C_{max} ($\mu\text{g/mL}$)	$T_{1/2}$ (days)
31	94 (modeled)	23.2	1.9

CONCLUSIONS

- AKY-1189's discovery exemplifies the synergy of biological (YSD) and medicinal chemistry optimization to a radiopharmaceutical clinical candidate.
- AKY-1189 has been engineered for high-affinity and specificity for Nectin-4 as well as a favorable pharmacokinetic profile and reduced renal retention.
- ²²⁵Ac-AKY-1189 drives robust anti-tumor responses in translationally relevant models of metastatic urothelial carcinoma after a single dose while displaying improved anti-tumor effects compared to three doses of enfortumab vedotin.
- AKY-1189 labeled with either ⁶⁸Ga (for PET/CT) or ¹⁷⁷Lu (for SPECT/CT) has been evaluated in a first in human imaging assessment. **For details, please attend the presentation of Abstract #10 on Friday, October 25, 2024.**
- ²²⁵Ac-AKY-1189 is a first-in-class Nectin-4 miniprotein-based radiopharmaceutical discovered at Aktis Oncology, which is progressing towards IND filing.

ACKNOWLEDGEMENTS

We thank Ved Srivastava (Perpetual Medicines) and Chris Baht and James Bowman (AI Proteins and formerly from Institute for Protein Innovation) for their contributions to this work.



REFERENCES

- Fabre-Lafay S, Monville F, Garrido-Urbani S, et al. Nectin-4 is a new histological and serological tumor associated marker for breast cancer. *BMC Cancer*. 2007;7(73).
- Takano A, Ishikawa N, Nishino R, et al. Identification of nectin-4 oncoprotein as a diagnostic and therapeutic target for lung cancer. *Cancer Res*. 2009;69(16):6694-703.
- Rosenberg J, Sridhar SS, Zhang J, et al. EV-101: a phase I study of single-agent enfortumab vedotin in patients with nectin-4-positive solid tumors, including metastatic urothelial carcinoma. *J Clin Oncol*. 2020;38(10):1041-1049.
- Sanders C, Lau J-F, Dietrich D, et al. Nectin-4 is widely expressed in head and neck squamous cell carcinoma. *Oncotarget*. 2022;13:1166-1173.
- Pill J, Kraenzlin B, Jander J, et al. Fluorescein-labeled sinistrin as marker of glomerular filtration rate. *Eur J Med Chem*. 2005;40(10):1056-61.
- Powles TB, Valderama BP, Gupta S, et al. Enfortumab vedotin and pembrolizumab in untreated advanced urothelial cancer. *N Engl J Med*. 2024;390:875-888.
- www.accessdata.fda.gov/drugsatfda_docs/nda/2019/761137Orig1s000MultiDisciplineR.pdf